Neuropharmacology 113 (2017) 490–501

Contents lists available at ScienceDirect

Neuropharmacology

journal homepage: www.elsevier.com/locate/neuropharm

TCF7L2 mediates the cellular and behavioral response to chronic lithium treatment in animal models

Katarzyna Misztal [a, 1], Nikola Brozko [a, b, c, 1], Andrzej Nagalski [a, b], Lukasz M. Szewczyk [a, c], Marta Krolak [d], Katarzyna Brzozowska [a, b, c], Jacek Kuznicki [a], Marta B. Wisniewska [a, b, *]

[a] International Institute of Molecular and Cell Biology, Laboratory of Neurodegeneration, Warsaw, Poland
[b] University of Warsaw, Centre of New Technologies, Laboratory of Molecular Neurobiology, Poland
[c] Postgraduate School of Molecular Medicine, Warsaw, Poland
[d] University of Warsaw, College of Inter-Faculty Individual Studies in Mathematics and Natural Sciences, Poland

ARTICLE INFO

Article history:
Received 6 October 2015
Received in revised form
20 October 2016
Accepted 24 October 2016
Available online 25 October 2016

Keywords:
Bipolar disorder
Lithium treatment
Wnt signaling
β-catenin
TCF7L2
Behavior

ABSTRACT

The mechanism of lithium's therapeutic action remains obscure, hindering the discovery of safer treatments for bipolar disorder. Lithium can act as an inhibitor of the kinase GSK3α/β, which in turn negatively regulates β-catenin, a co-activator of LEF1/TCF transcription factors. However, unclear is whether therapeutic levels of lithium activate β-catenin in the brain, and whether this activation could have a therapeutic significance. To address this issue we chronically treated mice with lithium. Although the level of non-phospho-β-catenin increased in all of the brain areas examined, β-catenin translocated into cellular nuclei only in the thalamus. Similar results were obtained when thalamic and cortical neurons were treated with a therapeutically relevant concentration of lithium *in vitro*. We tested if TCF7L2, a member of LEF1/TCF family that is highly expressed in the thalamus, facilitated the activation of β-catenin. Silencing of *Tcf7l2* in thalamic neurons prevented β-catenin from entering the nucleus, even when the cells were treated with lithium. Conversely, when *Tcf7l2* was ectopically expressed in cortical neurons, β-catenin shifted to the nucleus, and lithium augmented this process. Lastly, we silenced *tcf7l2* in zebrafish and exposed them to lithium for 3 days, to evaluate whether TCF7L2 is involved in the behavioral response. Lithium decreased the dark-induced activity of control zebrafish, whereas the activity of zebrafish with *tcf7l2* knockdown was unaltered. We conclude that therapeutic levels of lithium activate β-catenin selectively in thalamic neurons. This effect is determined by the presence of TCF7L2, and potentially contributes to the therapeutic response.

1. Introduction

An estimated 1.5–6% of the adult population is affected by bipolar disorder (BD), characterized by alternations between depressive and manic episodes of different lengths and intensities (Hilty et al., 2006). The first-line therapy to stabilize mood is lithium due to its prophylactic and acute effectiveness, although the mechanism of its therapeutic action is still under investigation (Freland and Beaulieu, 2012). Unfortunately, the margin between these beneficial effects and severe toxicity is small, thus necessitating investigations of new treatments (Kinahan et al., 2014). To discover targets for alternative mood stabilizers, the molecular mechanisms that underlie the therapeutic effects of lithium must be ascertained.

Three direct targets of lithium ions have been extensively studied: inositol monophosphate phosphatase (IMPA1 and IMPA2), glycogen synthase kinase 3 (GSK3α and -β), and the signaling complex of AKT kinase, β-arrestin 2, and protein phosphatase 2A (PP2A) (Beaulieu and Caron, 2008; O'Brien and Klein, 2009). Lithium inhibits IMPA and GSK3 by competing with magnesium ions, which is a cofactor for these enzymes (Ryves and Harwood, 2001). The inhibition of IMPA leads to reduction of available inositol and downstream targets of inositol cycle, which in turn decrease the release of calcium, diacylglycerol activation and protein kinase C activity (Berridge, 1984). In the case of the AKT/β-arrestin 2/PP2A complex, lithium prevents its formation and the

* Corresponding author. University of Warsaw, Centre of New Technologies, Laboratory of Molecular Neurobiology, ul. Banacha 2C, 02-097 Warsaw, Poland.
E-mail address: m.wisniewska@uw.edu.pl (M.B. Wisniewska).
[1] Contributed equally.

http://dx.doi.org/10.1016/j.neuropharm.2016.10.027

subsequent inactivation of AKT by PP2A (Freland and Beaulieu, 2012). AKT inhibits GSK3 by phosphorylating it at serine 9/21, providing an additional mechanism of the lithium-dependent inhibition of GSK3.

Studies with genetically modified mice have supported the hypothesis that GSK3 is a target of lithium in the treatment of BD. GSK3β haploinsufficiency or the deletion of GSK3β in D2R-expressing neurons mimicked lithium treatment in induced models of depression and mania (O'Brien et al., 2004; Urs et al., 2012), whereas the ectopic expression of a constitutively active GSK3β mutant or overexpression of GSK3β reversed lithium-sensitive behavior (O'Brien et al., 2011; Prickaerts et al., 2006). However, one issue is whether the therapeutic concentrations of lithium in serum and the brain (i.e., 0.5–1.5 mM) (Beaulieu et al., 2008; Guelen et al., 1992; Oruch et al., 2014; Soares et al., 2001) can actually exert an inhibitory effect on GSK3 because it requires 3–10 times higher levels to see the effect in cell-based assays (Kremer et al., 2011). Furthermore, a question emerges, what are the downstream therapeutic targets of lithium and GSK3?

One of the targets of GSK3 is β-catenin, a mediator of the canonical Wnt signaling pathway. GSK3 phosphorylates β-catenin at serine 33/37 in a destruction complex that also comprises adenomatous polyposis coli (APC) and AXIN1/2. When phosphorylated, β-catenin can be degraded *via* the proteasome pathway. The stimulation of cells with a canonical WNT ligand leads to rearrangement of the complex and the release of non-phosphorylated β-catenin, followed by the translocation of β-catenin to the nucleus where it acts in tandem with lymphoid enhancer-binding factor 1/T-cell factors (LEF1/TCF) to regulate gene transcription (Archbold et al., 2012). In mammals, the TCF/LEF family includes LEF1, TCF7, TCF7L1 and TCF7L2. The mechanism of the cytoplasmic-nuclear redistribution of β-catenin is not fully understood. Some studies implicated β-catenin binding partners, particularly TCF/LEF transcription factors, in β-catenin nuclear-cytoplasmic shuttling or retention (Henderson, 2000; Henderson et al., 2002; Huber et al., 1996; Jamieson et al., 2011; Krieghoff et al., 2006; Rosin-Arbesfeld et al., 2003; Schmitz et al., 2011; Tolwinski and Wieschaus, 2001; Wiechens and Fagotto, 2001). The physiological implications and possible regulatory role of this mechanism have not yet been confirmed.

β-catenin is critically involved in embryonic patterning and stem cell proliferation and differentiation, including nervous system development (Bengoa-Vergniory and Kypta, 2015; Braun et al., 2003; Hsu et al., 2015; Lie et al., 2005; Luo and Huang, 2016; Nouri et al., 2015; Schafer et al., 2015; Zechner et al., 2003). The nuclear localization of β-catenin is also observed in neurons in the adult brain but only in the thalamus and medial habenula in the diencephalon, and tectum in the midbrain (Misztal et al., 2011; Nagalski et al., 2013; Wisniewska et al., 2010). TCF7L2 is also specifically expressed in these brain regions (Nagalski et al., 2013). The precise role of β-catenin and TCF7L2 in adult brain function is still elusive (Wisniewska, 2013), nevertheless recent evidence suggests that TCF7L2/β-catenin play a role in the thalamus in determining the final identity of thalamic neurons (Nagalski et al., 2016) and driving expression of genes that regulate neuronal excitability (Wisniewska et al., 2010, 2012). β-catenin could play a role in the regulation of anxiety-related behavior. For example, transgenic mice that express a stabilized form of β-catenin in neurons exhibited a decrease in immobility time in the forced swim test and attenuation of amphetamine-induced hyperlocomotion (Gould et al., 2007).

In the present study, we used a mouse and zebrafish model of chronic lithium treatment and primary neuronal cultures to determine whether lithium, at concentrations that are considered to be therapeutic in humans, can activate β-catenin (i.e., induce its stabilization and nuclear translocation) in the brain. Although lithium at a high concentration (10 mM) activated β-catenin in different types of neurons, β-catenin shifted to the nucleus at a therapeutically relevant concentration (1 mM) only in thalamic neurons, both *in vivo* and *in vitro*. This selective action of lithium appeared to occur through the TCF7L2-dependent nuclear accumulation of β-catenin, which operates in thalamic neurons. The silencing of *tcf7l2* in zebrafish antagonized the effect of lithium on dark-induced locomotion, suggesting the involvement of TCF7L2 in the behavioral response to lithium treatment.

2. Materials and methods

2.1. Animal handling

C57BL/6 mice (male, 8–9 weeks old) were housed under standard conditions with food and water available *ad libitum*. Breeding zebrafish (*Danio rerio*) of the ABxTL line were maintained at 28 °C on a 14 h light/10 h dark cycle (Brand et al., 2002). The embryos were staged according to Kimmel et al. (1995). All of the experiments were approved by the Polish local Ethical Committee No. 1 in Warsaw (approval no. 275/2012).

2.2. Lithium administration in mice

The mice were given LiCl by intraperitoneal injections (2 mmol/kg body weight in a volume of 100 μl) for 14 days or in drinking water (600 mg/L) for 7–11 days. Control mice were injected with physiological saline or given pure drinking water, respectively. After the mice were sacrificed by cervical translocation, blood samples were immediately collected from the heart.

2.3. Lithium measurement

Lithium ions concentrations in murine serum and brain samples, and in whole zebrafish were measured by inductively coupled plasma mass spectrometry (ICP-MS) in the Central Chemical Laboratory of the Polish Geological Institute.

2.4. Total protein extraction and subcellular fractionation

For total protein extracts brain fragments were sectioned, and the tissue was immediately homogenized in cold lysis buffer (20 mM Tris [pH 6.8], 0.1 M NaCl, 2 mM EDTA [pH 8.0], 10% glycerol, 1% TritonX-100, 0.5 mM DTT, 1 mM PMSF, and protease and phosphatase inhibitors) with a Potter-Elvehjem homogenizer. For subcellular protein fractions brain fragments were immediately homogenized in buffer A (10 mM HEPES [pH 7.9], 1.5 mM $MgCl_2$, 10 mM NaCl, 0.5 mM DTT, 0.5 mM PMSF, and protease inhibitors) with a Potter-Elvehjem homogenizer followed by a passage through a 26-gauge needle and then centrifuged at 1000×*g* for 10 min. Afterward, the supernatants and pellets were processed separately. The supernatants were centrifuged at 100,000×*g* for 1 h to separate cytosolic and membrane fractions. Supernatant/cytosolic fractions were collected, and pellets/membranes were resuspended in buffer M (10 mM Tris [pH 7.4], 1 mM EDTA [pH 8.0], 1 mM EGTA [pH 8.0], 150 mM NaCl, 0.5% Triton X-100, 0.1% NP-40, and protease and phosphatase inhibitors). In parallel, the 1000×*g* pellets, representing cell nuclei and debris, were resuspended in 3 vol of buffer B (20 mM HEPES [pH 7.9], 1.5 mM $MgCl_2$, 600 mM NaCl, 0.5 mM DTT, 0.2 mM EDTA [pH 8.0], 0.5 mM PMSF, and protease inhibitors) and incubated for 30 min with gentle shaking to release nuclear proteins. The samples were then centrifuged at 25,000×*g* for 30 min, and the collected supernatants were further centrifuged at 100,000×*g* for 30 min to remove debris and membrane

fragments. The final supernatants represented nuclear fractions. All of the steps of the isolation procedure were performed at 4 °C.

2.5. Semi-quantitative Western blot

Concentrations of proteins in the extracts were measured using the Bradford assay (Bio-Rad), and equal amounts (10–20 μg) were separated on 10% sodium dodecyl sulfate-polyacrylamide gel electrophoresis gels. The following primary antibodies were used: rabbit anti-β-catenin (1:500; Santa Cruz Biotechnology), rabbit anti-non-phospho (active) β-catenin (Ser33/37/Thr41, 1:500; Cell Signaling), mouse anti-NeuN (1:1000; Millipore), rabbit anti-GAPDH (1:250; Santa Cruz Biotechnology), mouse anti-Pan-cadherin (1:1000; Abcam), and rabbit anti-HSP90 (1:1000; Enzo Life Sciences). Two types of secondary antibodies were used, depending on a subsequent visualization method: antibodies coupled with fluorophores IRDye 800CW or IRDye 680RD (1:10,000; LI-COR Biosciences) for the Odyssey Infrared Imaging System (LI-COR Biosciences), and antibodies coupled with horseradish peroxidase (HRP; 1:10,000; Sigma Aldrich) for the ImageQuant LAS 4000 system (GE Healthcare Life Sciences). In the latter case, the chemiluminescent reaction with luminol, cumaric acid, and hydrogen peroxide was performed with membranes stained with primary and secondary antibodies. The intensity or density of the detected bands was quantified using Image Studio 1.1 software (LI-COR Biosciences) or ImageQuant TL 7.0 software (GE Healthcare Life Sciences), respectively.

2.6. Primary neuronal cultures

Dissociated primary thalamic and cortical cultures were prepared from embryonic day 19 rat brains and cultured according to procedures described previously (Misztal et al., 2011). The Polish local Ethical Committee No. 1 in Warsaw approved the procedure. To reduce glial cell growth in thalamic cultures, 2.5 μM AraC was added to the medium for 24 h on the day after seeding. The neurons were grown in Neurobasal medium supplemented with B27 (Gibco), 0.5 mM glutamine, 12.5 mM glutamate, and penicillin/streptomycin (Sigma Aldrich). All of the cultures were maintained at 37 °C in a humidified atmosphere with 5% CO_2.

2.7. Cell transfection

Thalamic neurons on 4 days *in vitro* (4 DIV) were transfected with 0.4 μg empty pCG plasmid plus 0.1 μg green fluorescent protein (GFP) expression plasmid pCMV-GFP and 0.25 μg *Tcf7l2*-specific short-hairpin RNA (shRNA) expression plasmid per well. The shRNA sequences were the following: shRNA 1 (5-CACCTCCGCACTTACCAGC-3), shRNA 2 (5-CTCCGAAAGTTTCCGAGAT-3), and shRNA 3 (5-CACACATCGTTTCGAACAA-3). These sequences were designed using siRNA Selection Server (Yuan et al., 2004). The control shRNA (5-CCTAAGGTTAAGTCGCCCT-3) did not match any rodent mRNA sequence (Karalay et al., 2011). All of the oligonucleotides were cloned into pSUPER plasmids. Neurobasal medium (50 μl) and 1.5 μl of Lipofectamine 2000 (Invitrogen) were added to the DNA, gently mixed, and incubated for 25 min at room temperature. The media from the cells were collected and replaced by media without antibiotics and without glutamate. The DNA mixtures were then added to the cells for 4 h. Afterward, the cells were washed and kept in the medium that was collected before transfection. After 72 h, the cell cultures were fixed.

2.8. Cell transduction

Recombinant adenoviruses were prepared using the AdEasy Adenoviral Vector System (Agilent Technologies). For GFP and TCF7L2 overexpression, pShuttle vector was modified by inserting a truncated RSV promoter, woodchuck post-transcriptional regulatory element (WPRE), and SV-40 polyadenylation signal sequence as previously described (Boulos et al., 2006). TCF7L2-S3 isoform cDNA was subcloned from pCG-TCF7L2-S3 plasmid into a modified pShuttle vector. Viruses were generated from pShuttle vectors using a standard procedure described elsewhere (Luo et al., 2007), followed by purification using the Vivapure AdenoPACK 20 kit (Sartorius) and titration with the AdEasy Viral Titer Kit (Agilent Technologies), yielding approximately 10^{10} infection units/ml. The viral stocks were maintained at −80 °C before use. On 4 DIV of the neuronal culture, half of the culture media was removed, and purified virus was added to each well at 100 MOI (multiplicity of infection) and incubated for 6 h at 37 °C. The virus solution was then removed and replaced by fresh neuronal culture media. After 72 h, the cells were treated with 10 mM lithium chloride or PBS for 6 h and then fixed.

2.9. Cell treatment

For proteasome inhibition, 10 μM MG132 (Sigma Aldrich) or dimethylsulfoxide (DMSO; as a control) were added for 14 h before fixation to 7 DIV thalamic neurons. For GSK3 inhibition, 1 and 10 mM LiCl or PBS (as a control) were added for 6 h before fixation. For Wnt activation, WNT3A (50 ng/ml) was added for 6 h before fixation.

2.10. Immunofluorescent cell staining

The immunofluorescence analysis was performed as described previously (Misztal et al., 2011). Briefly, the cells were incubated overnight with rabbit anti-β-catenin antibody (1:250; Santa Cruz Biotechnology) in a humidified chamber and then for 1.5 h at room temperature with mouse anti-TCF7L2 antibody (1:1000; EMD Millipore). The secondary antibodies [anti-mouse and anti-rabbit IgG coupled with AlexaFluor 488, 568, or 674 (Invitrogen, Molecular Probes, Eugene)] were applied for 45 min at room temperature. All of the antibodies were diluted in 2% bovine serum albumin. The images were acquired using a Zeiss LSM5 Exciter confocal microscope. The levels of nuclear and cytoplasmic β-catenin and TCF7L2 (mean grey values for fluorescence intensity) were measured using ImageJ software followed by manually selecting intracellular regions of interest (ROIs). Equal contrast and brightness enhancement were used for the images shown in the figures.

2.11. Morpholino injection

The *tcf7l2* Morpholino (MO, Gene Tools) was injected into one-cell stage wild type (WT) embryos in the concentration of 4 ng/μl. The Morpholino binds to the first exon and first intron (5′-CTTATTTGTCACTTACCTCGGAATC-3′). WT embryos injected with water were used as a control.

2.12. Exposure of zebrafish larvae to lithium

Two days after the morpholino injections, the zebrafish larvae received 5 mM NaCl (control), or 1 and 5 mM LiCl dissolved in standard E3 medium for zebrafish embryos. The plates were maintained at 28.5 °C. Lithium ions concentrations in zebrafish were measured by ICP-MS.

2.13. Dark-induced locomotion test

All of the testing was performed at a temperature of 25 °C after 1

p.m. to ensure steady activity of the zebrafish larvae. The locomotor activity assays were performed using a ViewPoint behavior recording system (Zebrabox) and appropriate software. The evening before locomotor activity assessment, the larvae were individually placed in a 24-well plate. WT and morphant zebrafish larvae that were immersed in ±1000 μl of E3 medium, 1 mM LiCl or 5 mM LiCl were placed together on each plate. Thirty minutes before the experiment, the larvae were moved to the behavioral testing room to adapt to the new conditions. The larvae were placed in a Zebrabox for 5 min for acclimation under the neutral light of 50–65 lux and then larva movements were measured under the following lighting conditions: 10 min under the neutral light or 10 min in the dark proceeded by 10 min of the bright light (400 lux). For each experiment three plates were measured in triplicates. The distance traveled (cm) in the dark per unit time (min) per larva was calculated and served as a measure of locomotor activity.

2.14. Zebrafish forebrain section preparation and immunofluorescence

The larvae were collected and fixed in 4% paraformaldehyde in PBS at 4 °C overnight. The following day they were transferred to PBS that contained 30% sucrose for equilibration and maintained at 4 °C. The larvae were then embedded in Tissue-Tek O.C.T. (Optimal Cutting Temperature)compound (Sakura Finetek), kept at −80 °C for 20 min for rapid-freezing and stored at −20 °C. Frozen blocks were coronally sectioned into 20-μm slices using Leica CM1850 cryostat (Leica Microsystems). The sections were sealed to the glass slides, washed three times with PBS and 0.2% Triton X-100 (PBS-T) for 10 min each, and blocked for 1 h with 1% bovine serum albumin, and 2% normal donkey serum in 0.5% PBS-T. The sections were then incubated overnight at 4 °C with primary antibodies in humidity chamber. The following primary antibodies were used: mouse anti-TCF7L2 (1:100, EMD Millipore) and rabbit anti-β-catenin (1:100, Santa Cruz Biotechnology). After incubation the sections were washed twice in PBS for 20 min, and once in 0.2% PBS-T and then incubated with the secondary antibodies for 2 h. The following secondary antibodies were used: anti-rabbit and anti-mouse immunoglobulin G coupled with AlexaFluor 488 and 594. Staining intensity was observed under Zeiss Axio Imager Z2 LSM700 confocal microscope.

2.15. Statistical analysis

The statistical analyses were performed using *t*-test, one-way ANOVA or two-way ANOVA followed by Tukey post hoc test. Values of $p < 0.05$ were considered statistically significant. The data were analyzed using GraphPad software. In case of behavioral experiments, the resulting data was initially tested to evaluate distribution and homogeneity. In all cases the number of animals tested is denoted by *n*. Standard deviation is denoted by SD and standard error of the mean by SEM. Statistical significance was depicted as follows: ns – non significant, $^{*}p < 0.05$, $^{**}p < 0.01$, $^{***}p < 0.001$.

3. Results

3.1. Chronic lithium treatment activates the GSK3/β-catenin pathway in the forebrain, but β-catenin accumulates in cell nuclei only in the thalamus

We used a mouse model to determine if the GSK3/β-catenin pathway is activated in the brain by chronic lithium at therapeutically-relevant concentrations (Supplementary Fig. S1; Supplementary Materials and Methods). The treatment was optimized to obtain lithium concentration in the brain and blood between 0.5 mM and 1.5 mM. Mice that exhibited serum lithium concentration <0.5 mM and >1.5 mM were excluded from further analyses. The activity of the GSK3/β-catenin pathway was assessed by the level of active β-catenin (ABC) (Staal et al., 2002), i.e., N-terminal non-phosphorylated β-catenin, in the thalamus, hippocampus, and cortex (the dorsal part). ABC levels increased at least two-fold in the thalamus and hippocampus when the mice were administered lithium (Fig. 1A), indicating that in these brain region GSK3 was inhibited. In the cortex the increase was smaller and was statistically insignificant.

The increase in ABC suggested that β-catenin was stabilized and could translocate into cellular nuclei in the brain. To verify it, we fractionated tissues of three areas of the forebrain – the thalamus, hippocampus, and cortex (the dorsal part) – and measured β-catenin levels in cytoplasmic and nucleoplasmic fractions using a semi-quantitative infrared-based Western blot method. Because the abundance of membrane-attached β-catenin (β-catenin is a bifunctional protein that is also involved in cell-cell adhesion; Valenta et al., 2012) could contaminate other fractions and contribute to false results, we first optimized the fractionation method using hippocampal homogenates and analyzed the purity of the fractions using the soluble proteins GAPDH and HSP90, membrane protein cadherins, and the neuron-specific nuclear protein NeuN (Fig. 1B). In the cytosolic fraction, we detected only the soluble proteins. In the nuclear fraction, we detected the soluble proteins and NeuN. In the membrane fraction, we detected cadherins, in addition to the soluble proteins and NeuN. Thus, membranous proteins did not contaminate the cytosolic or nuclear fractions. Nuclear proteins did not contaminate the cytosolic fraction, and the nuclear fraction was highly enriched in nuclear proteins. We considered this to be satisfactory purity.

We then compared the levels of β-catenin between hippocampal and thalamic fractions from untreated mice (Fig. 1C). β-catenin was easily detected in the membranes from the thalamus and hippocampus, and in the cytosol and nucleosol from the thalamus. In the cytosol and nucleosol from the hippocampus, only a weak β-catenin signal was detected. These results were supported by our previous immunohistochemical data, which showed β-catenin immunoreactivity in neuropils throughout the brain, including the thalamus and hippocampus, and in neural cell bodies in the entire thalamus but not hippocampus, cortex or striatum (Nagalski et al., 2013; Wisniewska et al., 2010).

We then compared the levels of β-catenin between control and lithium-treated mice in the cytosol and nucleosol of cells from the thalamus, hippocampus, and cortex. The cytoplasmic and nuclear levels of β-catenin did not change in the cortex, but the treatment evoked an approximately two-fold increase in β-catenin in the cytosolic fraction from the hippocampus and nuclear fraction from the thalamus (Fig. 1D). We also analyzed the subcellular localization of β-catenin in the brain in lithium-treated mice by immunohistochemistry, to see if β-catenin was activated in any other areas of the brain. However, sensitivity of this method did not allow detecting low levels of β-catenin in the cytoplasm or nuclei in areas outside the thalamus. Therefore we could only say that apart from the thalamus massive nuclear translocation of β-catenin did not occur in the brain in the chronically treated mice (Supplementary Fig. S2).

Concluding, β-catenin was apparently stabilized in hippocampal and thalamic cells by chronic lithium treatment, but its accumulation was observed only in the nuclei of thalamic neurons, where it could carry out its function as a transcription cofactor.

3.2. Nuclear localization of β-catenin in thalamic neurons is determined by TCF7L2

We next sought to determine why only thalamic neurons

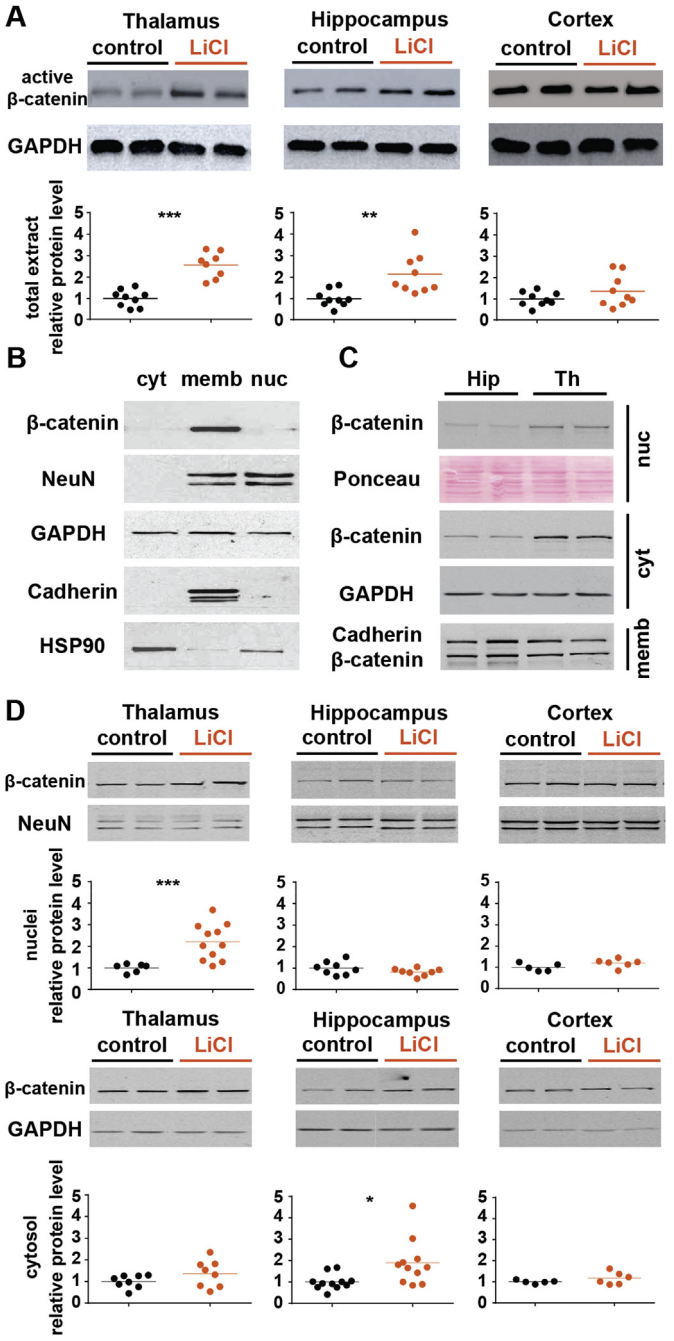

Fig. 1. Subcellular fractionation of brain tissue and nuclear and cytosolic β-catenin levels in the brain in control and lithium-treated mice. (A) Western blot analysis of active β-catenin in total extracts from the thalamus, hippocampus and cortex. GAPDH staining was used as a loading control. (B) Western blot detection of β-catenin and markers of the cytosol, membranes, and nuclei in subcellular fractions of the hippocampus. β-catenin was observed in the membranes but not in the nuclear or cytosolic fractions. (C) β-catenin levels in subcellular fractions of the hippocampus and thalamus. Hip, hippocampus (mice 1 and 2); Th, thalamus. (D) Western blot analysis of β-catenin levels in two representative samples of the nuclear and cytosolic fractions from the thalamus, hippocampus and cortex. NeuN and GAPDH staining was used as a loading control. Each dot represents one animal. Horizontal lines indicate mean values, and error bars indicate SD. $^{*}p < 0.05$, $^{**}p < 0.01$, $^{***}p < 0.001$ (two-tailed *t*-test).

exhibited β-catenin accumulation in the nuclear compartment. Our previous research showed that TCF7L2 is specifically expressed in the thalamus and midbrain (Nagalski et al., 2013), and evidence from other studies showed that TCF/LEF proteins are able to shift β-catenin to the nuclei in several cell lines (Huber et al., 1996; Jamieson et al., 2011; Krieghoff et al., 2006). These findings led us to hypothesize that TCF7L2 might be involved in the nuclear localization of β-catenin in the thalamus. To test this hypothesis, we used primary neuronal cultures as an experimental model.

Thalamic neurons *in vitro* include a mixture of TCF7L2-positive and TCF7L2-negative neurons (Misztal et al., 2011). Using immunofluorescence analysis, we first demonstrated the nuclear localization of β-catenin in thalamic neurons only in TCF7L2-positive cells (Fig. 2A). To investigate whether the subcellular localization of β-catenin in these cells depends on TCF7L2, we silenced the *Tcf7l2* gene using RNA interference. We designed three different Tcf7l2-specific shRNAs and showed that all of them, but not the control shRNA, effectively decreased the level of TCF7L2, as revealed by immunofluorescence analysis. We observed a drop of nuclear β-catenin staining in the cells in which *Tcf7l2* was silenced (Fig. 2B and C). We next ectopically expressed either TCF7L2 or GFP (as a control) in cortical cultures. Immunofluorescence revealed a shift of β-catenin into the nuclei in TCF7L2-expressing cells (Fig. 2D and E). In contrast, β-catenin localized only to the plasma membrane in control neurons.

To further investigate the role of TCF7L2 in the nuclear localization of β-catenin in thalamic neurons, we stabilized the free pool of β-catenin by treating the cells with the proteasome inhibitor MG132 for 14 h and then analyzed its subcellular localization (Fig. 3A and B). In both TCF7L2-positive and TCF7L2-negative neurons, β-catenin accumulated in the cytoplasm upon MG132 treatment. However, in TCF7L2-negative cells, the ratio of nuclear-to-cytoplasmic β-catenin levels was 0.5 and did not change upon MG132 treatment, whereas the ratio was 0.8 and increased to 1.3 when β-catenin was stabilized in TCF7L2-positive cells (Fig. 3C). Thus, regardless of how high the level of β-catenin was in the cytoplasm, β-catenin accumulated in the nuclei only in TCF7L2-positive cells, confirming that the nuclear shift of β-catenin in thalamic neurons is primarily regulated by TCF7L2 and not by its stabilization.

3.3. Susceptibility of neurons to the lithium-evoked nuclear accumulation of β-catenin depends on TCF7L2

To assess whether the effect of lithium treatment also depends on the presence of TCF7L2, cultured thalamic neurons were treated for 6 h with 1 mM LiCl, which corresponds to therapeutically relevant doses *in vivo*, or 10 mM LiCl that is usually used in a cell based assays (Kremer et al., 2011) (Fig. 4A–C). In TCF7L2-positive cells, 1 mM lithium was sufficient to induce the nuclear accumulation of β-catenin in thalamic cells, which was consistent with the *in vivo* results (Fig. 1D). In contrast, in TCF7L2-negative neurons, β-catenin levels increased in the cytoplasm upon 1 mM lithium treatment, but the shift to the nuclei was observed only when we increased lithium concentration to 10 mM. This suggests a key role for TCF7L2 in the susceptibility of thalamic neurons to the lithium-evoked nuclear accumulation of β-catenin.

We next examined the effects of lithium on β-catenin in cortical neurons that ectopically expressed TCF7L2 or GFP as a control. Treatment with 1 mM LiCl did not affect the cytoplasmic or nuclear levels of β-catenin in control cortical neurons in culture (Fig. 4D–F), which was consistent with the *in vivo* findings for the cortex (Fig. 1D). However, when TCF7L2 was expressed, β-catenin accumulated in the nucleus, and its level further increased in the presence of lithium. In this case, 1 mM lithium was also sufficient to evoke the nuclear shift of β-catenin. In both, TCF7L2 expressing and non-expressing cortical neurons, 10 mM LiCl evoked β-catenin shift to the nucleus, as expected, though only in the presence of TCF7L2 we observed substantial accumulation of β-catenin. Similar results were obtained when neurons were treated with the WNT3A

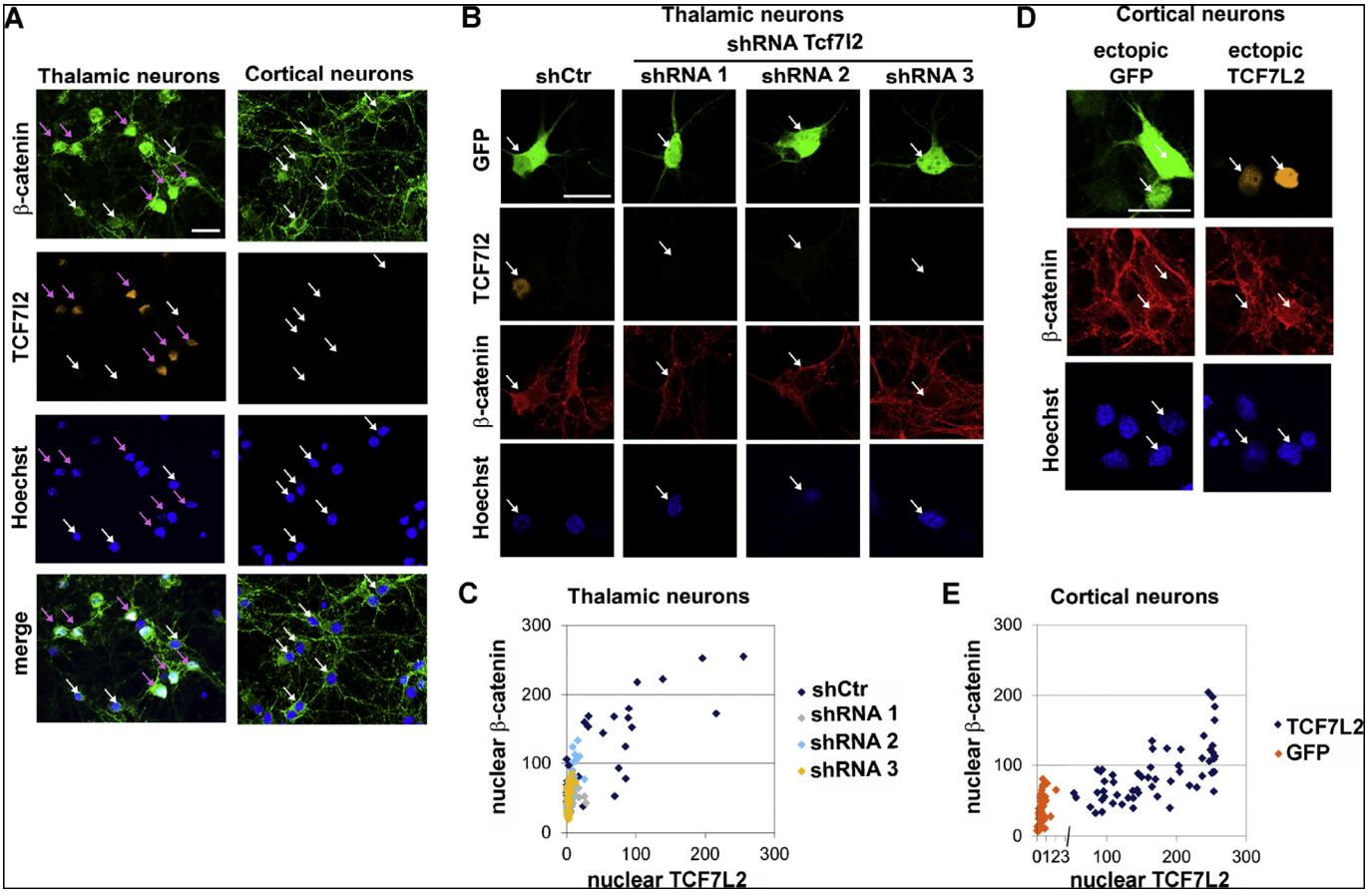

Fig. 2. TCF7L2 drives β-catenin to the nuclei in neurons. (A) Immunofluorescent staining of thalamic and cortical neurons with anti-β-catenin antibody (green), anti-TCF7L2 antibody (orange), and counterstaining with Hoechst (blue). Pink and white arrows point to neurons that are positive and negative for nuclear β-catenin and TCF7L2, respectively. (B) Thalamic neurons were transfected with control or *Tcf7l2*-specific shRNA vectors and co-transfected with a GFP vector to visualize transfected neurons (green). The cells were stained with anti-TCF7L2 antibody (orange), anti-β-catenin antibody (red), and Hoechst (blue). The arrows point to transfected neurons. (C) Scatter plots of β-catenin and TCF7L2 staining intensities in thalamic neurons. Each dot represents one neuron. (D) Cortical neurons were transduced with either GFP (green) or TCF7L2 adenoviral vectors. The cells were stained with anti-TCF7L2 antibody (orange), anti-β-catenin antibody (red), and Hoechst (blue). The arrows point to infected neurons. Scale bars = 20 μm. (E) Scatter plots of β-catenin and TCF7L2 staining intensities in cortical neurons. Each dot represents one neuron.

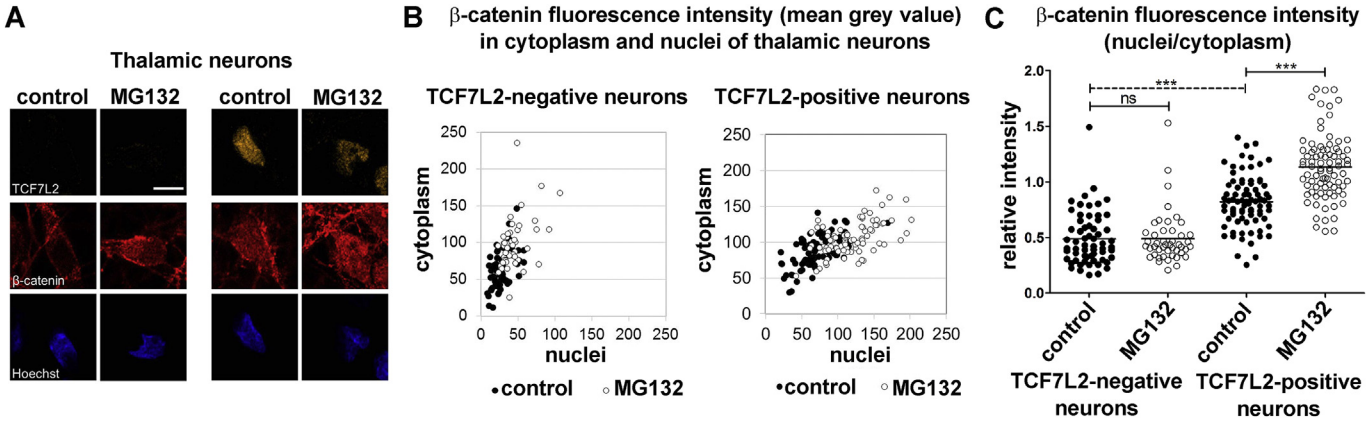

Fig. 3. Stabilization of β-catenin in thalamic neurons is followed by its nuclear shift only when TCF7L2 is expressed. (A) Thalamic neurons were treated with 10 μM MG132 or drug vehicle (DMSO; as a control) for 14 h. The cells were stained with anti-TCF7L2 antibody (orange), anti-β-catenin antibody (red), and Hoechst (blue). Scale bar = 10 μm. (B) Two-scatter plot of intensity values for β-catenin staining in the nucleus and cytoplasm of TCF7L2-positive and -negative thalamic neurons treated with DMSO as a control (black) or MG132 (white). Each dot represents a single cell. (C) Graph representing the ratio of β-catenin fluorescence values (in arbitrary units) in the nucleus to the values in the cytoplasm. Each dot represents a single cell. Horizontal lines indicate mean values. ***$p < 0.001$ (one-way ANOVA followed by Tukey post hoc test). (For interpretation of the references to colour in this figure legend, the reader is referred to the web version of this article.)

protein (Supplementary Fig. S3). Altogether, these results demonstrated that in thalamic neurons β-catenin shifted to the nucleus by therapeutically-relevant concentrations of lithium, whereas cortical neurons were resistant, unless TCF7L2 was ectopically expressed.

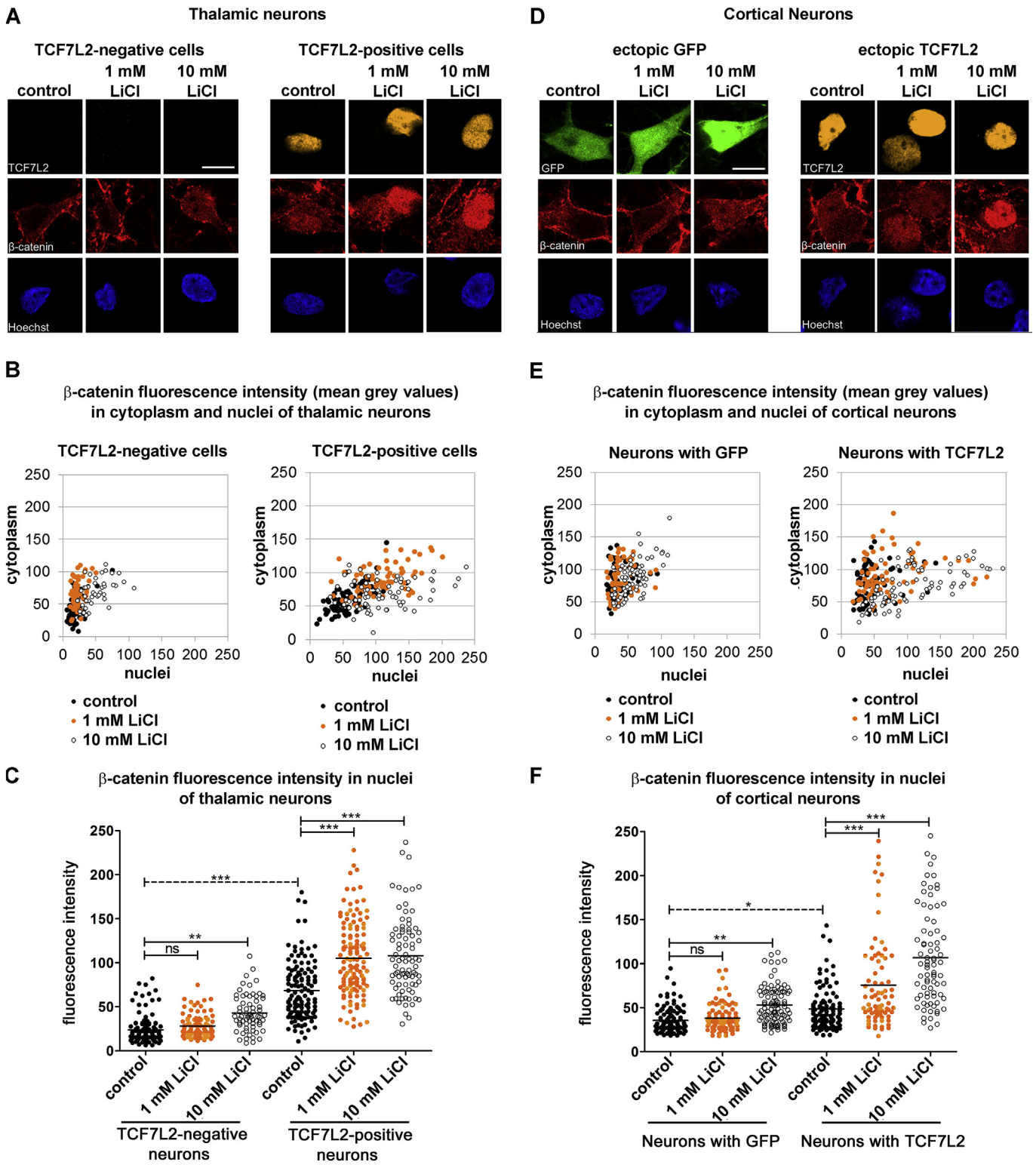

Fig. 4. Sensitivity of neurons to lithium depends on the presence of TCF7L2. (A) Thalamic neurons were treated for 6 h with PBS (control) or 1 or 10 mM LiCl and then fixed and stained with anti-TCF7L2 antibody (orange), anti-β-catenin antibody (red), and Hoechst (blue). (B) Graph representing the values of β-catenin fluorescence intensity in the nucleus and cytoplasm of TCF7l2-positive and -negative thalamic neurons under control conditions (black) and upon LiCl treatment: 1 mM (orange) and 10 mM (white). (C) Graph representing β-catenin fluorescence values in the nucleus in thalamic neurons. Each dot represents a single cell (at least 65 cells were counted for each condition in two independent experiments). Horizontal lines indicate mean values. (D) Cortical neurons were transduced with adenoviral vectors that expressed either GFP (left panel) or TCF7L2 (right panel) and treated for 6 h with PBS (control) or 1 or 10 mM LiCl. GFP-expressing cells are green, and anti-TCF7L2 antibody-stained cells are orange. The cells were stained with anti-β-catenin antibody (red), and the nuclei were stained with Hoechst (blue). Scale bar = 10 μm. (E) Graph representing the values of β-catenin fluorescence intensity in the nucleus and cytoplasm of cortical neurons transduced with GFP or a TCF7L2 expression vector under control conditions (black) or upon 1 mM (orange) or 10 mM (white) LiCl treatment. (F) Graph representing β-catenin fluorescence values in the nucleus in cortical cells. Each dot represents a single cell (at least 70 cells were counted for each condition in two independent experiments). Horizontal lines indicate mean values. $^{*}p < 0.05$, $^{**}p < 0.01$, $^{***}p < 0.001$ (one-way ANOVA followed by Tukey post hoc test).

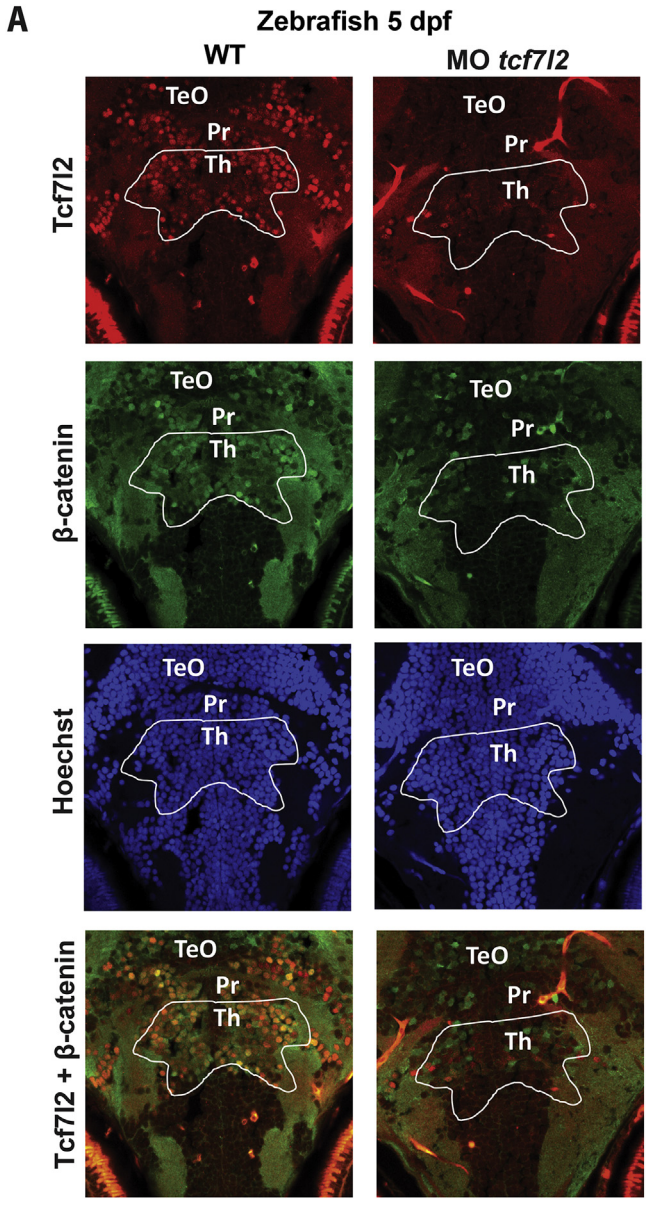

3.4. The behavioral changes of zebrafish in response to lithium treatment depend on the presence of TCF7L2

Lastly, we investigated whether TCF7L2 is involved in the behavioral response to lithium. Because *Tcf7l2*−/− mice are not viable because of the defective proliferation of crypt stem cells in the small intestine (Korinek et al., 1998), we used zebrafish that subsist on yolk lipids by the first 5 days post fertilization (5 dpf) when the brain is fully formed. In zebrafish, *tcf7l2* is expressed in the thalamus, habenula, and tectum (Young et al., 2002), similar to observations in mice or rats. Tcf7l2-deficient zebrafish develop fairly normally up to six weeks (Muncan et al., 2007). Importantly, the main divisions of the diencephalon (i.e., the thalamus and habenula) as well as *tcf7l2* expression patterns in the zebrafish brain resemble those in mammals (Nagalski et al., 2013; Young et al., 2002).

We knocked down *tcf7l2* in zebrafish using splice-blocking morpholino oligonucleotides. We first analyzed morpholino efficiency. Western blot revealed a dose-dependent decrease in Tcf7l2 levels in 3 dpf larvae (Supplementary Fig. S4). We decided to use the 4 ng dose, which was characterized by a high Tcf7l2 depletion and negligible side effects. Successful Tcf7l2 depletion was confirmed by immunofluorescence sections from 5 dpf of morphant zebrafish (Fig. 5A). Importantly, in WT zebrafish larvae Tcf7l2 and β-catenin were present in the nuclei of thalamic neurons, similar to observations in mice. We then examined whether Tcf7l2 influences the nuclear localization of β-catenin in the zebrafish thalamus. Immunofluorescent staining revealed β-catenin in cell nuclei in the thalamus in WT larvae but not in *tcf7l2* morphants (Fig. 5A), which was consistent with our cell culture studies (Fig. 2B), indicating that Tcf7l2 is needed for the nuclear localization of β-catenin also in zebrafish.

To investigate whether Tcf7l2 depletion attenuates lithium-sensitive behavior, we exposed WT and Tcf7l2-deficient zebrafish to 1 and 5 mM LiCl for 2.5 days. The concentrations of lithium in the zebrafish body at the end of this period were 0.4 mmol/kg and 2 mmol/kg, respectively (measured by ICP-MS). On 5 dpf, larvae were evaluated for dark-induced locomotor activity. This test has been previously shown to measure the level of anxiety-like behavior in zebrafish larvae (Burgess and Granato, 2007; Steenbergen et al., 2011) and responses to lithium and other mood stabilizers (Chen et al., 2015; Egan et al., 2009; Irons et al., 2010; Nery et al., 2014). Locomotor activity was measured as the distance traveled over a 10 min-period in the dark. Under the neutral light morphant larvae traveled about twice shorter distance than WT larvae (Fig. 5B), but sudden darkness induced a three-fold increase in the locomotion in both morphant and WT larvae. We found that induced locomotor activity gradually decreased in WT zebrafish larvae as the concentration of LiCl increased (Fig. 5B), whereas the average distances traveled by WT larvae that were immersed in E3 medium or medium supplemented with 5 mM NaCl were not different. Larvae that were treated with 1 and 5 mM

Fig. 5. Silencing of *tcf7l2* in zebrafish decreases the level of nuclear β-catenin in thalamic neurons and attenuates the behavioral response to LiCl in zebrafish larvae. (A) Zebrafish brain slices were stained immunohistochemically with anti-TCF7L2 antibody (red), anti-β-catenin antibody (green), and counterstained with Hoechst nuclear dye (blue). TeO – optic tectum, Pr – pretectum, Th – thalamus. (B) *tcf7l2* morphant zebrafish larvae were exposed to LiCl at 2 dpf for 2.5 days, and thereafter dark-induced locomotion was measured. The chart represents the distance traveled by zebrafish larvae during 10 min in the dark or under the neutral light under the following conditions – 5 mM NaCl, E3 medium, 1 mM LiCl, and 5 mM LiCl. The colors of bars indicate different groups of larvae, black – WT, grey – morphants. ****$p < 0.0001$, *$p < 0.05$ (two-way ANOVA followed by Tukey post hoc test). Error bars indicate SEM ($n = 23–34$).

LiCl traveled approximately 20% and 40% shorter distance, respectively. In contrast, locomotor activity did not change in morphant zebrafish, regardless of the LiCl concentration (Fig. 5B). A two-way ANOVA test showed that the silencing of *tcf7l2* had a statistically significant effect on the behavioral response to lithium ($p = 0.0027$ for the interaction).

4. Discussion

Lithium, which is known to inhibit GSK3, is presumed to activate β-catenin in the brain when it is taken as a mood stabilizer for the treatment of BD, but research that may support this hypothesis has been surprisingly scarce. Our results demonstrated that β-catenin accumulation in thalamic neurons depends on high levels of TCF7L2 protein in the thalamus and is potentiated by therapeutic concentrations of lithium. This TCF7L2-dependent effect influences the behavioral response of lithium treatment in zebrafish and might contribute to the therapeutic effects of this mood stabilizer.

The possibility that GSK3 in the brain can be inhibited by lithium at therapeutic concentrations has been questioned (Phiel and Klein, 2001). A challenge in addressing this issue is the lack of methods to detect GSK3 activity *in vivo* (Hur and Zhou, 2010), and one possibility is to examine the phosphorylation of its targets. In the present study, we examined changes in the phosphorylation status of the GSK3 substrate β-catenin. Lithium treatment increased the level of N-terminal non-phosphorylated β-catenin, also called active β-catenin, in the thalamus and hippocampus, demonstrating the inhibition of GSK3 in these parts of the brain. This active form of β-catenin is usually assumed to ultimately translocate into the nucleus, but previous research on β-catenin signaling has focused on undifferentiated cells and cancer cells, which, by nature, readily respond to canonical Wnt signaling. Our results demonstrate that such phenomena apparently do not occur in neurons. A shift of β-catenin into the nucleus was observed only in thalamic cells, what was further confirmed in primary thalamic and cortical neuronal cultures that were treated with different concentrations of lithium.

Previous studies reported activation of β-catenin in the hippocampus, amygdala and hypothalamus in chronically treated mice with lithium (Gould et al., 2004; O'Brien et al., 2004). These results, however, raises some technical questions. In the study of Gould et al., β-catenin levels were measured in so-called soluble fractions (Gould et al., 2004), which in fact represented only cytosolic proteins and did not inform about the amount of β-catenin that actually translocated to the nucleus. In the study of O'Brien et al., β-catenin activity was determined by an *in vivo* reporter gene assay in transgenic mice with a β−galactosidase gene driven by β-catenin/TCF/LEF responsive promoter (O'Brien et al., 2004), but the authors themselves called their quantifications preliminary. Moreover, although TCF/LEF reporter transgenic mice exhibits a correct readout of β-catenin signaling during development and in cancer, the reliability of this approach in adult organs, including the brain, is much less certain (Al Alam et al., 2011; Barolo, 2006). Our results, showing no effect of lithium on the nuclear shift of β-catenin are consistent with a recent study (Mills et al., 2014), in which a stabilized form of β-catenin failed to accumulate in the nuclei of neurons in the hippocampus in transgenic mice.

We demonstrated that this specific potential of thalamic neurons to accumulate β-catenin in the nuclear compartment depends on high levels of TCF7L2 protein. This conclusion is based on the following data on neuronal primary cultures: (*i*) TCF7L2-positive thalamic neurons, but not cortical neurons that do not express endogenous TCF7L2 protein, showed nuclear β-catenin localization; (*ii*) gene silencing of *Tcf7l2* by RNA interference in thalamic neurons effectively decreased the level of nuclear β-catenin, whereas the ectopic expression of *Tcf7l2* in cortical neurons translocated β-catenin to the nuclei; and (*iii*) the stabilization of free β-catenin through proteasome inhibition in TCF7L2-positive and TCF7L2-negative thalamic neurons led to nuclear β-catenin accumulation only in TCF7L2-positive cells. Although, the ability of TCF/LEF proteins to shift β-catenin to cell nuclei was previously reported in established cell lines (Huber et al., 1996; Jamieson et al., 2011; Krieghoff et al., 2006), to our knowledge this is the first demonstration of the physiological significance of such a regulatory mechanism.

As demonstrated herein, the presence of TCF7L2 also predisposes thalamic neurons to the nuclear translocation of β-catenin upon treatment with a low concentration of lithium (1 mM), which closely approximates therapeutic levels in humans. In contrast, in cortical neurons, β-catenin was not detected in the nucleus unless a high lithium concentration (10 mM) was administered or *Tcf7l2* was ectopically expressed. Therefore, the presence of TCF7L2 changes the threshold for the lithium-evoked nuclear accumulation of β-catenin. Therapeutic lithium concentrations are sufficient to activate β-catenin in thalamic neurons, but such concentrations are below the threshold for other cells. The low level of the β-catenin destruction complex, which we reported previously (Misztal et al., 2011), might additionally contribute to the susceptibility of thalamic neurons to lithium. Cortical neurons that ectopically expressed TCF7L2 were more prone to β-catenin nuclear translocation after lithium treatment than control neurons, but they were still less sensitive than TCF7L2-positive neurons from the thalamus, which is consistent with these previous results. Therefore, we propose that the mechanism of the selective action of lithium on the thalamus at therapeutically relevant concentrations involves high levels of TCF7L2 and low levels of GSK3.

To test our hypothesis that TCF7L2-dependent activation of β-catenin is a part of the therapeutic response to lithium treatment, we performed a behavioral test in Tcf7l-deficient zebrafish. Importantly, many recent studies confirmed that zebrafish can be valuable for analyzing the behavioral effects of lithium (Nery et al., 2014) and other psychoactive drugs like D-amphetamine (Irons et al., 2010), fluoxetine (Egan et al., 2009), or lorazepam (Chen et al., 2015). It was shown that the sudden onset of darkness induces robust locomotor responses in zebrafish larvae, and this effect can be used to measure anxiety-like behavior (Burgess and Granato, 2007; Peng et al., 2016; Steenbergen et al., 2011). Our observation that lithium suppresses locomotor reaction to sudden darkness in WT larvae is consistent with a previous study (Nery et al., 2014). However, in the case of *tcf7l2* morphant larvae, lithium exposure did not change the locomotor response. This result suggests that lithium exerts at least some of its behavioral effects through the activation of TCF7L2-positive neurons, which are localized mainly in the thalamus and habenula (Nagalski et al., 2013).

How the thalamus and habenula could be related to neuropsychiatric disorders? Specific electrophysiological properties enable the thalamus to play a major role in directing attention and actively regulating information transmission to the cortex (Constantinople and Bruno, 2013; Min, 2010; Mitchell et al., 2014; Saalmann and Kastner, 2011). Unsurprisingly, the functioning of the thalamocortical loop have been shown to be impaired in schizophrenia, major depression, and BD (Anticevic et al., 2014a,b; Haijma et al., 2013; Laje et al., 2010; Miller et al., 2015; Pergola et al., 2015; Radenbach et al., 2010). It is known that habenular circuits regulate fear and anxiety both in mammals and teleost (Facchin et al., 2015; Heldt and Ressler, 2006; Lee et al., 2010; Mathuru and Jesuthasan, 2013; Pang et al., 2016; Pobbe and Zangrossi, 2008), and recent studies reported habenular pathologies in patients with BD and depression (Lawson et al., 2016; Savitz et al., 2011).

The TCF7L2-dependent effects of lithium in the thalamus might

be medically relevant because TCF7L2 has already been linked to psychiatric conditions. Variants of the *TCF7L2* gene were associated with schizophrenia and BD in candidate gene studies (Alkelai et al., 2012; Hansen et al., 2011; Winham et al., 2014), and *de novo* mutations in *TCF7L2* were found in autistic patients (Iossifov et al., 2014). Moreover, *Tcf7l2* haplo-insufficient mice exhibited anxiety-like phenotypes in behavioral studies (Savic et al., 2011). Previous studies from our group suggested that β-catenin, together with TCF/LEF transcription factors, shapes the intrinsic firing properties of thalamic neurons by regulating a group of genes that are involved in neuronal excitability (Wisniewska et al., 2010, 2012). In zebrafish, Tcf7l2 and Wnt signaling were shown to regulate differentiation of neurons in habenula (Beretta et al., 2013; Husken et al., 2014; Kuan et al., 2015), We speculate that β-catenin activity that is too low in thalamic (and habenular) neurons can result in the poor setting and adjustment of response firing modes and contribute to the pathophysiology of these neuropsychiatric conditions. Lithium, in turn, would restore stability of the thalamocortical and/or habenular system by increasing β-catenin activity and stabilizing the expression of β-catenin/TCF/LEF-dependent genes.

Beaulieu et al. proposed another scenario for the therapeutic action of lithium. According to these authors, lithium may restore the proper functioning of striatal dopaminergic neurons by interfering with dopamine D_2 receptor-dependent activation of the AKT/β-arrestin 2/PP2A complex and consequently inhibiting the AKT target GSK3 (Beaulieu et al., 2004). This possibility was strongly supported by the resistance of β-arrestin 2 knockout mice to lithium-induced behavioral changes (Beaulieu et al., 2008) and antipsychotic effects in mice with GSK3β deletion in D_2 receptor-expressing neurons (Urs et al., 2012). The downstream targets of dopamine/AKT/GSK3 signaling are currently unknown, but β-catenin is apparently not one of them (Urs et al., 2012). Our hypothesis of TCF7L2-dependent effects of lithium does not exclude AKT-mediated lithium's actions on striatal dopaminergic neurons. These two models instead may be complementary, especially with regard to other actions of lithium beyond antipsychotic effects. Both models imply the selective action of lithium on particular populations of neurons.

Concluding, TCF7L2 potentially mediates molecular effects of lithium in thalamic and possibly in habenular neurons by facilitating the activation of β-catenin, and contributes to behavioral responses to lithium. Hence, TCF7L2 might provide a link between lithium's actions, the thalamus and neuropsychiatric conditions. It also points to TCF7L2 and β-catenin as potential therapeutic targets in the treatment of mood disorders.

Conflict of interest

The authors declare no conflict of interest.

Author contributions

Design – KM, AN, MBW; experiments – KM, NB, AN, KB, MK, LMS; writing – KM, NB, AN, MBW, JK. All of the authors contributed to the data analysis/interpretation and critically reviewed the entire manuscript.

Acknowledgements

This work was supported by “NeuConnect” within the framework ERA-Net NEURON (grant no. 01EW1106) to JK, and by Polish National Science Centre (grant no. 2011/03/B/NZ3/04480) to MBW and (grant no. 2013/09/N/NZ3/01377) to NB. KM was supported by a “START” stipend from the Foundation for Polish Science. We thank Dariusz Lech from the Polish Institute of Geology for the lithium measurements and Dr. Tomasz Wegierski for critically reading the manuscript.

Appendix A. Supplementary data

Supplementary data related to this article can be found at http://dx.doi.org/10.1016/j.neuropharm.2016.10.027.

References

Al Alam, D., Green, M., Tabatabai Irani, R., Parsa, S., Danopoulos, S., Sala, F.G., Branch, J., El Agha, E., Tiozzo, C., Voswinckel, R., Jesudason, E.C., Warburton, D., Bellusci, S., 2011. Contrasting expression of canonical Wnt signaling reporters TOPGAL, BATGAL and Axin2(LacZ) during murine lung development and repair. PLoS One 6, e23139.

Alkelai, A., Greenbaum, L., Lupoli, S., Kohn, Y., Sarner-Kanyas, K., Ben-Asher, E., Lancet, D., Macciardi, F., Lerer, B., 2012. Association of the type 2 diabetes mellitus susceptibility gene, TCF7L2, with schizophrenia in an Arab-Israeli family sample. PLoS One 7, e29228.

Anticevic, A., Cole, M.W., Repovs, G., Murray, J.D., Brumbaugh, M.S., Winkler, A.M., Savic, A., Krystal, J.H., Pearlson, G.D., Glahn, D.C., 2014a. Characterizing thalamo-cortical disturbances in schizophrenia and bipolar illness. Cereb. Cortex 24, 3116–3130.

Anticevic, A., Yang, G., Savic, A., Murray, J.D., Cole, M.W., Repovs, G., Pearlson, G.D., Glahn, D.C., 2014b. Mediodorsal and visual thalamic connectivity differ in schizophrenia and bipolar disorder with and without psychosis history. Schizophr. Bull. 40, 1227–1243.

Archbold, H.C., Yang, Y.X., Chen, L., Cadigan, K.M., 2012. How do they do Wnt they do?: regulation of transcription by the Wnt/β-catenin pathway. Acta Physiol. (Oxf.) 204, 74–109.

Barolo, S., 2006. Transgenic Wnt/TCF pathway reporters: all you need is Lef? Oncogene 25, 7505–7511.

Beaulieu, J.M., Caron, M.G., 2008. Looking at lithium: molecular moods and complex behaviour. Mol. Interv. 8, 230–241.

Beaulieu, J.M., Sotnikova, T.D., Yao, W.D., Kockeritz, L., Woodgett, J.R., Gainetdinov, R.R., Caron, M.G., 2004. Lithium antagonizes dopamine-dependent behaviors mediated by an AKT/glycogen synthase kinase 3 signaling cascade. Proc. Natl. Acad. Sci. U. S. A. 101, 5099–5104.

Beaulieu, J.M., Marion, S., Rodriguiz, R.M., Medvedev, I.O., Sotnikova, T.D., Ghisi, V., Wetsel, W.C., Lefkowitz, R.J., Gainetdinov, R.R., Caron, M.G., 2008. A beta-arrestin 2 signaling complex mediates lithium action on behavior. Cell 132, 125–136.

Bengoa-Vergniory, N., Kypta, R.M., 2015. Canonical and noncanonical Wnt signaling in neural stem/progenitor cells. Cell Mol. Life Sci. 72, 4157–4172.

Beretta, C.A., Dross, N., Bankhead, P., Carl, M., 2013. The ventral habenulae of zebrafish develop in prosomere 2 dependent on Tcf7l2 function. Neural Dev. 8, 19.

Berridge, M.J., 1984. Inositol trisphosphate and diacylglycerol as second messengers. Biochem. J. 220, 345–360.

Boulos, S., Meloni, B.P., Arthur, P.G., Bojarski, C., Knuckey, N.W., 2006. Assessment of CMV, RSV and SYN1 promoters and the woodchuck post-transcriptional regulatory element in adenovirus vectors for transgene expression in cortical neuronal cultures. Brain Res. 1102, 27–38.

Brand, M., Granato, M., Nüsslein-Volhard, C., 2002. Keeping and raising zebrafish. In: Nüsslein-Volhard, C., Dahm, R. (Eds.), Zebrafish, a Practical Approach.

Braun, M.M., Etheridge, A., Bernard, A., Robertson, C.P., Roelink, H., 2003. Wnt signaling is required at distinct stages of development for the induction of the posterior forebrain. Development 130, 5579–5587.

Burgess, H.A., Granato, M., 2007. Modulation of locomotor activity in larval zebrafish during light adaptation. J. Exp. Biol. 210, 2526–2539.

Chen, F., Chen, S., Liu, S., Zhang, C., Peng, G., 2015. Effects of lorazepam and WAY-200070 in larval zebrafish light/dark choice test. Neuropharmacology 95, 226–233.

Constantinople, C.M., Bruno, R.M., 2013. Deep cortical layers are activated directly by thalamus. Science 340, 1591–1594.

Egan, R.J., Bergner, C.L., Hart, P.C., Cachat, J.M., Canavello, P.R., Elegante, M.F., Elkhayat, S.I., Bartels, B.K., Tien, A.K., Tien, D.H., Mohnot, S., Beeson, E., Glasgow, E., Amri, H., Zukowska, Z., Kalueff, A.V., 2009. Understanding behavioral and physiological phenotypes of stress and anxiety in zebrafish. Behav. Brain Res. 205, 38–44.

Facchin, L., Duboue, E.R., Halpern, M.E., 2015. Disruption of epithalamic left-right asymmetry increases anxiety in zebrafish. J. Neurosci. 35, 15847–15859.

Freland, L., Beaulieu, J.M., 2012. Inhibition of GSK3 by lithium, from single molecules to signaling networks. Front. Mol. Neurosci. 5, 14.

Gould, T.D., Chen, G., Manji, H.K., 2004. In vivo evidence in the brain for lithium inhibition of glycogen synthase kinase-3. Neuropsychopharmacology 29, 32–38.

Gould, T.D., O'Donnell, K.C., Picchini, A.M., Manji, H.K., 2007. Strain differences in lithium attenuation of d-amphetamine-induced hyperlocomotion: a mouse model for the genetics of clinical response to lithium.

Neuropsychopharmacology 32, 1321–1333.
Guelen, P.J., Janssen, T.J., De Witte, T.C., Vree, T.B., Benson, K., 1992. Bioavailability of lithium from lithium citrate syrup versus conventional lithium carbonate tablets. Biopharm. Drug Dispos. 13, 503–511.
Haijma, S.V., Van Haren, N., Cahn, W., Koolschijn, P.C., Hulshoff Pol, H.E., Kahn, R.S., 2013. Brain volumes in schizophrenia: a meta-analysis in over 18 000 subjects. Schizophr. Bull. 39, 1129–1138.
Hansen, T., Ingason, A., Djurovic, S., Melle, I., Fenger, M., Gustafsson, O., Jakobsen, K.D., Rasmussen, H.B., Tosato, S., Rietschel, M., Frank, J., Owen, M., Bonetto, C., Suvisaari, J., Thygesen, J.H., Petursson, H., Lonnqvist, J., Sigurdsson, E., Giegling, I., Craddock, N., O'Donovan, M.C., Ruggeri, M., Cichon, S., Ophoff, R.A., Pietilainen, O., Peltonen, L., Nothen, M.M., Rujescu, D., St Clair, D., Collier, D.A., Andreassen, O.A., Werge, T., 2011. At-risk variant in TCF7L2 for type II diabetes increases risk of schizophrenia. Biol. Psychiatry 70, 59–63.
Heldt, S.A., Ressler, K.J., 2006. Lesions of the habenula produce stress- and dopamine-dependent alterations in prepulse inhibition and locomotion. Brain Res. 1073–1074, 229–239.
Henderson, B.R., 2000. Nuclear-cytoplasmic shuttling of APC regulates beta-catenin subcellular localization and turnover. Nat. Cell Biol. 2, 653–660.
Henderson, B.R., Galea, M., Schuechner, S., Leung, L., 2002. Lymphoid enhancer factor-1 blocks adenomatous polyposis coli-mediated nuclear export and degradation of beta-catenin. Regulation by histone deacetylase 1. J. Biol. Chem. 277, 24258–24264.
Hilty, D.M., Leamon, M.H., Lim, R.F., Kelly, R.H., Hales, R.E., 2006. A review of bipolar disorder in adults. Psychiatry (Edgmont) 3, 43–55.
Hsu, L.C., Nam, S., Cui, Y., Chang, C.P., Wang, C.F., Kuo, H.C., Touboul, J.D., Chou, S.J., 2015. Lhx2 regulates the timing of beta-catenin-dependent cortical neurogenesis. Proc. Natl. Acad. Sci. U. S. A. 112, 12199–12204.
Huber, O., Korn, R., McLaughlin, J., Ohsugi, M., Herrmann, B.G., Kemler, R., 1996. Nuclear localization of beta-catenin by interaction with transcription factor LEF-1. Mech. Dev. 59, 3–10.
Hur, E.M., Zhou, F.Q., 2010. GSK3 signalling in neural development. Nat. Rev. Neurosci. 11, 539–551.
Husken, U., Stickney, H.L., Gestri, G., Bianco, I.H., Faro, A., Young, R.M., Roussigne, M., Hawkins, T.A., Beretta, C.A., Brinkmann, I., Paolini, A., Jacinto, R., Albadri, S., Dreosti, E., Tsalavouta, M., Schwarz, Q., Cavodeassi, F., Barth, A.K., Wen, L., Zhang, B., Blader, P., Yaksi, E., Poggi, L., Zigman, M., Lin, S., Wilson, S.W., Carl, M., 2014. Tcf7l2 is required for left-right asymmetric differentiation of habenular neurons. Curr. Biol. 24, 2217–2227.
Iossifov, I., O'Roak, B.J., Sanders, S.J., Ronemus, M., Krumm, N., Levy, D., Stessman, H.A., Witherspoon, K.T., Vives, L., Patterson, K.E., Smith, J.D., Paeper, B., Nickerson, D.A., Dea, J., Dong, S., Gonzalez, L.E., Mandell, J.D., Mane, S.M., Murtha, M.T., Sullivan, C.A., Walker, M.F., Waqar, Z., Wei, L., Willsey, A.J., Yamrom, B., Lee, Y.H., Grabowska, E., Dalkic, E., Wang, Z., Marks, S., Andrews, P., Leotta, A., Kendall, J., Hakker, I., Rosenbaum, J., Ma, B., Rodgers, L., Troge, J., Narzisi, G., Yoon, S., Schatz, M.C., Ye, K., McCombie, W.R., Shendure, J., Eichler, E.E., State, M.W., Wigler, M., 2014. The contribution of de novo coding mutations to autism spectrum disorder. Nature 515, 216–221.
Irons, T.D., MacPhail, R.C., Hunter, D.L., Padilla, S., 2010. Acute neuroactive drug exposures alter locomotor activity in larval zebrafish. Neurotoxicol. Teratol. 32, 84–90.
Jamieson, C., Sharma, M., Henderson, B.R., 2011. Regulation of beta-catenin nuclear dynamics by GSK-3beta involves a LEF-1 positive feedback loop. Traffic 12, 983–999.
Karalay, O., Doberauer, K., Vadodaria, K.C., Knobloch, M., Berti, L., Miquelajauregui, A., Schwark, M., Jagasia, R., Taketo, M.M., Tarabykin, V., Lie, D.C., Jessberger, S., 2011. Prospero-related homeobox 1 gene (Prox1) is regulated by canonical Wnt signaling and has a stage-specific role in adult hippocampal neurogenesis. Proc. Natl. Acad. Sci. U. S. A. 108, 5807–5812.
Kimmel, C.B., Ballard, W.W., Kimmel, S.R., Ullmann, B., Schilling, T.F., 1995. Stages of embryonic development of the zebrafish. Dev. Dyn. 203, 253–310.
Kinahan, J.C., NiChorcorain, A., Cunningham, S., Freyne, A., Cooney, C., Barry, S., Kelly, B.D., 2014. Risk factors for polyuria in a cross-section of community psychiatric lithium-treated patients. Bipolar Disord. 17, 50–62.
Korinek, V., Barker, N., Moerer, P., van Donselaar, E., Huls, G., Peters, P.J., Clevers, H., 1998. Depletion of epithelial stem-cell compartments in the small intestine of mice lacking Tcf-4. Nat. Genet. 19, 379–383.
Kremer, A., Louis, J.V., Jaworski, T., Van Leuven, F., 2011. GSK3 and Alzheimer's disease: facts and fiction. Front. Mol. Neurosci. 4, 17.
Krieghoff, E., Behrens, J., Mayr, B., 2006. Nucleo-cytoplasmic distribution of beta-catenin is regulated by retention. J. Cell Sci. 119, 1453–1463.
Kuan, Y.S., Roberson, S., Akitake, C.M., Fortuno, L., Gamse, J., Moens, C., Halpern, M.E., 2015. Distinct requirements for Wntless in habenular development. Dev. Biol. 406, 117–128.
Laje, G., Cannon, D.M., Allen, A.S., Klaver, J.M., Peck, S.A., Liu, X., Manji, H.K., Drevets, W.C., McMahon, F.J., 2010. Genetic variation in HTR2A influences serotonin transporter binding potential as measured using PET and [11C]DASB. Int. J. Neuropsychopharmacol. 13, 715–724.
Lawson, R.P., Nord, C.L., Seymour, B., Thomas, D.L., Dayan, P., Pilling, S., Roiser, J.P., 2016. Disrupted habenula function in major depression. Mol. Psychiatry (Epub ahead of print).
Lee, A., Mathuru, A.S., Teh, C., Kibat, C., Korzh, V., Penney, T.B., Jesuthasan, S., 2010. The habenula prevents helpless behavior in larval zebrafish. Curr. Biol. 20, 2211–2216.
Lie, D.C., Colamarino, S.A., Song, H.J., Desire, L., Mira, H., Consiglio, A., Lein, E.S., Jessberger, S., Lansford, H., Dearie, A.R., Gage, F.H., 2005. Wnt signalling regulates adult hippocampal neurogenesis. Nature 437, 1370–1375.
Luo, S.X., Huang, E.J., 2016. Dopaminergic neurons and brain reward pathways: from neurogenesis to circuit assembly. Am. J. Pathol. 186, 478–488.
Luo, J., Deng, Z.L., Luo, X., Tang, N., Song, W.X., Chen, J., Sharff, K.A., Luu, H.H., Haydon, R.C., Kinzler, K.W., Vogelstein, B., He, T.C., 2007. A protocol for rapid generation of recombinant adenoviruses using the AdEasy system. Nat. Protoc. 2, 1236–1247.
Mathuru, A.S., Jesuthasan, S., 2013. The medial habenula as a regulator of anxiety in adult zebrafish. Front. Neural Circuits 7, 99.
Miller, C.H., Hamilton, J.P., Sacchet, M.D., Gotlib, I.H., 2015. Meta-analysis of functional neuroimaging of major depressive disorder in youth. JAMA Psychiatry 72, 1045–1053.
Mills, F., Bartlett, T.E., Dissing-Olesen, L., Wisniewska, M.B., Kuznicki, J., Macvicar, B.A., Wang, Y.T., Bamji, S.X., 2014. Cognitive flexibility and long-term depression (LTD) are impaired following beta-catenin stabilization in vivo. Proc. Natl. Acad. Sci. U. S. A. 111, 8631–8636.
Min, B.K., 2010. A thalamic reticular networking model of consciousness. Theor. Biol. Med. Model. 7, 10.
Misztal, K., Wisniewska, M.B., Ambrozkiewicz, M., Nagalski, A., Kuznicki, J., 2011. WNT protein-independent constitutive nuclear localization of {beta}-catenin protein and its low degradation rate in thalamic neurons. J. Biol. Chem. 286, 31781–31788.
Mitchell, A.S., Sherman, S.M., Sommer, M.A., Mair, R.G., Vertes, R.P., Chudasama, Y., 2014. Advances in understanding mechanisms of thalamic relays in cognition and behavior. J. Neurosci. 34, 15340–15346.
Muncan, V., Faro, A., Haramis, A.P., Hurlstone, A.F., Wienholds, E., van Es, J., Korving, J., Begthel, H., Zivkovic, D., Clevers, H., 2007. T-cell factor 4 (Tcf7l2) maintains proliferative compartments in zebrafish intestine. EMBO Rep. 8, 966–973.
Nagalski, A., Irimia, M., Szewczyk, L., Ferran, J.L., Misztal, K., Kuznicki, J., Wisniewska, M.B., 2013. Postnatal isoform switch and protein localization of LEF1 and TCF7L2 transcription factors in cortical, thalamic, and mesencephalic regions of the adult mouse brain. Brain Struct. Funct. 218, 1531–1549.
Nagalski, A., Puelles, L., Dabrowski, M., Wegierski, T., Kuznicki, J., Wisniewska, M.B., 2016. Molecular anatomy of the thalamic complex and the underlying transcription factors. Brain Struct. Funct. 221, 2493–2510.
Nery, L.R., Eltz, N.S., Martins, L., Guerim, L.D., Pereira, T.C., Bogo, M.R., Vianna, M.R., 2014. Sustained behavioral effects of lithium exposure during early development in zebrafish: involvement of the Wnt-beta-catenin signaling pathway. Prog. Neuropsychopharmacol. Biol. Psychiatry 55, 101–108.
Nouri, N., Patel, M.J., Joksimovic, M., Poulin, J.F., Anderegg, A., Taketo, M.M., Ma, Y.C., Awatramani, R., 2015. Excessive Wnt/beta-catenin signaling promotes midbrain floor plate neurogenesis, but results in vacillating dopamine progenitors. Mol. Cell Neurosci. 68, 131–142.
O'Brien, W.T., Harper, A.D., Jove, F., Woodgett, J.R., Maretto, S., Piccolo, S., Klein, P.S., 2004. Glycogen synthase kinase-3beta haploinsufficiency mimics the behavioral and molecular effects of lithium. J. Neurosci. 24, 6791–6798.
O'Brien, W.T., Klein, P.S., 2009. Validating GSK3 as an in vivo target of lithium action. Biochem. Soc. Trans. 37, 1133–1138.
O'Brien, W.T., Huang, J., Buccafusca, R., Garskof, J., Valvezan, A.J., Berry, G.T., Klein, P.S., 2011. Glycogen synthase kinase-3 is essential for beta-arrestin-2 complex formation and lithium-sensitive behaviors in mice. J. Clin. Invest. 121, 3756–3762.
Oruch, R., Elderbi, M.A., Khattab, H.A., Pryme, I.F., Lund, A., 2014. Lithium: a review of pharmacology, clinical uses, and toxicity. Eur. J. Pharmacol. 740C, 464–473.
Pang, X., Liu, L., Ngolab, J., Zhao-Shea, R., McIntosh, J.M., Gardner, P.D., Tapper, A.R., 2016. Habenula cholinergic neurons regulate anxiety during nicotine withdrawal via nicotinic acetylcholine receptors. Neuropharmacology 107, 294–304.
Peng, X., Lin, J., Zhu, Y., Liu, X., Zhang, Y., Ji, Y., Yang, X., Guo, N., Li, Q., 2016. Anxiety-related behavioral responses of pentylenetetrazole-treated zebrafish larvae to light-dark transitions. Pharmacol. Biochem. Behav. 145, 55–65.
Pergola, G., Selvaggi, P., Trizio, S., Bertolino, A., Blasi, G., 2015. The role of the thalamus in schizophrenia from a neuroimaging perspective. Neurosci. Biobehav. Rev. 54, 57–75.
Phiel, C.J., Klein, P.S., 2001. Molecular targets of lithium action. Annu. Rev. Pharmacol. Toxicol. 41, 789–813.
Pobbe, R.L., Zangrossi Jr., H., 2008. Involvement of the lateral habenula in the regulation of generalized anxiety- and panic-related defensive responses in rats. Life Sci. 82, 1256–1261.
Prickaerts, J., Moechars, D., Cryns, K., Lenaerts, I., van Craenendonck, H., Goris, I., Daneels, G., Bouwknecht, J.A., Steckler, T., 2006. Transgenic mice overexpressing glycogen synthase kinase 3beta: a putative model of hyperactivity and mania. J. Neurosci. 26, 9022–9029.
Radenbach, K., Flaig, V., Schneider-Axmann, T., Usher, J., Reith, W., Falkai, P., Gruber, O., Scherk, H., 2010. Thalamic volumes in patients with bipolar disorder. Eur. Arch. Psychiatry Clin. Neurosci. 260, 601–607.
Rosin-Arbesfeld, R., Cliffe, A., Brabletz, T., Bienz, M., 2003. Nuclear export of the APC tumour suppressor controls beta-catenin function in transcription. EMBO J. 22, 1101–1113.
Ryves, W.J., Harwood, A.J., 2001. Lithium inhibits glycogen synthase kinase-3 by competition for magnesium. Biochem. Biophys. Res. Commun. 280, 720–725.
Saalmann, Y.B., Kastner, S., 2011. Cognitive and perceptual functions of the visual thalamus. Neuron 71, 209–223.
Savic, D., Distler, M.G., Sokoloff, G., Shanahan, N.A., Dulawa, S.C., Palmer, A.A.,

Nobrega, M.A., 2011. Modulation ofTcf7l2 expression alters behavior in mice. PLoS One 6, e26897.
Savitz, J.B., Nugent, A.C., Bogers, W., Roiser, J.P., Bain, E.E., Neumeister, A., Zarate Jr., C.A., Manji, H.K., Cannon, D.M., Marrett, S., Henn, F., Charney, D.S., Drevets, W.C., 2011. Habenula volume in bipolar disorder and major depressive disorder: a high-resolution magnetic resonance imaging study. Biol. Psychiatry 69, 336–343.
Schafer, S.T., Han, J., Pena, M., von Bohlen Und Halbach, O., Peters, J., Gage, F.H., 2015. The Wnt adaptor protein ATP6AP2 regulates multiple stages of adult hippocampal neurogenesis. J. Neurosci. 35, 4983–4998.
Schmitz, Y., Wolkenhauer, O., Rateitschak, K., 2011. Nucleo-cytoplasmic shuttling of APC can maximize beta-catenin/TCF concentration. J. Theor. Biol. 279, 132–142.
Soares, J.C., Boada, F., Spencer, S., Mallinger, A.G., Dippold, C.S., Wells, K.F., Frank, E., Keshavan, M.S., Gershon, S., Kupfer, D.J., 2001. Brain lithium concentrations in bipolar disorder patients: preliminary (7)Li magnetic resonance studies at 3 T. Biol. Psychiatry 49, 437–443.
Staal, F.J., Noort Mv, M., Strous, G.J., Clevers, H.C., 2002. Wnt signals are transmitted through N-terminally dephosphorylated beta-catenin. EMBO Rep. 3, 63–68.
Steenbergen, P.J., Richardson, M.K., Champagne, D.L., 2011. Patterns of avoidance behaviours in the light/dark preference test in young juvenile zebrafish: a pharmacological study. Behav. Brain Res. 222, 15–25.
Tolwinski, N.S., Wieschaus, E., 2001. Armadillo nuclear import is regulated by cytoplasmic anchor Axin and nuclear anchor dTCF/Pan. Development 128, 2107–2117.
Urs, N.M., Snyder, J.C., Jacobsen, J.P., Peterson, S.M., Caron, M.G., 2012. Deletion of GSK3beta in D2R-expressing neurons reveals distinct roles for beta-arrestin signaling in antipsychotic and lithium action. Proc. Natl. Acad. Sci. U. S. A. 109, 20732–20737.
Valenta, T., Hausmann, G., Basler, K., 2012. The many faces and functions of beta-catenin. EMBO J. 31, 2714–2736.
Wiechens, N., Fagotto, F., 2001. CRM1- and Ran-independent nuclear export of beta-catenin. Curr. Biol. 11, 18–27.
Winham, S.J., Cuellar-Barboza, A.B., Oliveros, A., McElroy, S.L., Crow, S., Colby, C., Choi, D.S., Chauhan, M., Frye, M., Biernacka, J.M., 2014. Genome-wide association study of bipolar disorder accounting for effect of body mass index identifies a new risk allele in TCF7L2. Mol. Psychiatry 19, 1010–1016.
Wisniewska, M.B., 2013. Physiological role of beta-catenin/TCF signaling in neurons of the adult brain. Neurochem. Res. 38, 1144–1155.
Wisniewska, M.B., Misztal, K., Michowski, W., Szczot, M., Purta, E., Lesniak, W., Klejman, M.E., Dabrowski, M., Filipkowski, R.K., Nagalski, A., Mozrzymas, J.W., Kuznicki, J., 2010. LEF1/{beta}-Catenin complex regulates transcription of the Cav3.1 calcium channel gene (Cacna1g) in thalamic neurons of the adult brain. J. Neurosci. 30, 4957–4969.
Wisniewska, M.B., Nagalski, A., Dabrowski, M., Misztal, K., Kuznicki, J., 2012. Novel beta-catenin target genes identified in thalamic neurons encode modulators of neuronal excitability. BMC Genomics 13, 635.
Young, R.M., Reyes, A.E., Allende, M.L., 2002. Expression and splice variant analysis of the zebrafish tcf4 transcription factor. Mech. Dev. 117, 269–273.
Yuan, B., Latek, R., Hossbach, M., Tuschl, T., Lewitter, F., 2004. siRNA Selection Server: an automated siRNA oligonucleotide prediction server. Nucleic Acids Res. 32, W130–W134.
Zechner, D., Fujita, Y., Hulsken, J., Muller, T., Walther, I., Taketo, M.M., Crenshaw 3rd, E.B., Birchmeier, W., Birchmeier, C., 2003. beta-Catenin signals regulate cell growth and the balance between progenitor cell expansion and differentiation in the nervous system. Dev. Biol. 258, 406–418.